Journal Pre-proof


# BACTERIOCIN ENTEROCIN CRL35 is a modular peptide that induces non-bilayer states in bacterial model membranes

Carolina Medina Amado, Carlos J. Minahk, Eduardo Cilli, Rafael G. Oliveira, Fernando G. Dupuy

PII: S0005-2736(19)30283-4

DOI: https://doi.org/10.1016/j.bbamem.2019.183135

Reference: BBAMEM 183135

To appear in: *BBA - Biomembranes*

Received date: 28 June 2019

Revised date: 7 October 2019

Accepted date: 4 November 2019

Please cite this article as: C.M. Amado, C.J. Minahk, E. Cilli, et al., BACTERIOCIN ENTEROCIN CRL35 is a modular peptide that induces non-bilayer states in bacterial model membranes, *BBA - Biomembranes*(2019), https://doi.org/10.1016/j.bbamem.2019.183135

# BACTERIOCIN ENTEROCIN CRL35 IS A MODULAR PEPTIDE THAT INDUCES NON-BILAYER STATES IN BACTERIAL MODEL MEMBRANES

Carolina Medina Amado[a]; Carlos J. Minahk [a]; Eduardo Cilli [b]; Rafael G. Oliveira[c]; Fernando G. Dupuy[a, 1]

[a]Instituto Superior de Investigaciones Biológicas (INSIBIO) CONICET-UNT and Instituto de Química Biológica "Dr Bernabé Bloj", Facultad de Bioquímica, Química y Farmacia, Universidad Nacional de Tucumán. Chacabuco 461, T4000ILI, San Miguel de Tucumán, Tucumán, Argentina. Tel: +54-381-4248921

[b]Instituto de Química, UNESP, Universidad Estadual Paulista. Rua Prof. Francisco Degni, 55 Araraquara, 14800-060, São Paulo.

[c]Instituto de Investigaciones en Química Biológica de Córdoba (CIQUIBIC) CONICET-Departamento de Química Biológica Ranwel Caputto, Facultad de Ciencias Químicas, Universidad Nacional de Córdoba, Haya de la Torre y Medina Allende, Ciudad Universitaria, X5000HUA, Córdoba, Argentina.

[1] To whom correspondence should be addressed. fdupuy@fbqf.unt.edu.ar

**Abstract**

The mechanism of action of the anti-Listeria peptide enterocin CRL35 was studied with biophysical tools by using lipid mixtures that mimicked Gram-positive plasma membranes. Langmuir monolayers and infrared spectroscopy indicated that the peptide readily interacted with phospholipid assembled in monolayers and bilayers to produce a dual effect, depending on the acyl chains. Indeed, short chain mixtures were disordered by enterocin CRL35, but the gel-phases of membranes composed by longer acyl chains were clearly stabilized by the bacteriocin. Structural and functional studies indicated that non-bilayer states were formed when liposomes were co-incubated with enterocin CRL35, whereas significant permeabilization could be detected when bilayer and non-bilayer states co-existed. Results can be explained by a two-step model in which the N-terminal of the peptide firstly docks enterocin CRL35 on the lipid surface by means of electrostatic interactions; then, C-terminal triggers membrane perturbation by insertion of hydrophobic α-helix.

**Keywords**

BACTERIOCIN; BACTERIAL MEMBRANE; *LISTERIA*; X- RAY DIFFRACTION; MONOLAYER; SPECTROSCOPY

## 1. Introduction

Bacteriocins are antimicrobial peptides produced by bacteria, most of them active against phylogenetically related organisms. The class IIa includes linear peptides with no post-translational modifications [1,2]. These bacteriocins share some common features with other antimicrobial peptides, *i.e.*, multiple basic residues in the primary sequence and a strong affinity toward membranes of the sensitive microorganisms [3,4]. In this regard, the N-terminal was postulated to interact with a membrane receptor, the mannose transporter ManPTS; whereas the C terminal would be responsible of antimicrobial activity [5].

Enterocin CRL35 is a IIa bacteriocin of 43 residues produced by *Enterococcus mundtii* CRL35 that is active against the Gram-positive foodborne pathogen *Listeria monocytogenes* [6–8]. The mechanism of action is still under study and it's not clear whether the peptide is able to kill cells by itself or the receptor is necessary for the activity. Shorter peptides derived from enterocin sequence displayed diminished activity [9] but they were able to enhance the biological activity of the native peptide [6]. A hybrid chimera containing the enterocin CRL35 and the α-helix of the bitopic protein called EtpM, was constructed [10]. The purpose of that was to attach enterocin CRL35 to the Gram-negative *Escherichia coli* inner membranes, which do contain two phylogenetically distant ManPTS complexes that cannot bind pediocin-like bacteriocins [11]. The chimera showed activity against both Gram-positive *Listeria* cells as well as Gram-negative *Escherichia coli* [10]. Thus, although membrane receptors would be important for achieving antimicrobial selectivity at nanomolar concentrations, the capability of killing both types of cells suggests a mechanism of action involving non-specific cell membrane permeation.

Mechanism of action of antimicrobial peptides has been studied by several laboratories during many years, but a precise model explaining the sequence of events at a molecular level has been described for a few examples peptides so far and cannot, at the moment, be extended to the rest of antimicrobial peptides [12,13]. The barrel-stave mechanism was described for alamethicin at certain peptide:lipid mole ratio [14], whereas toroidal pore, made of both peptide and lipid molecules surrounding a pore in a bent interface, was described for mellitin [15,16]. Finding molecular determinants of peptide-membrane interactions is of high importance in order to identify critical features for a rational design of peptides with specific properties. In this regard, capabilities for membrane perturbation are of interest since membrane-based antimicrobial therapies are more difficult to avoid by bacteria than mechanisms based on protein targets, in which subtle single residue mutations can severely hamper interactions with antimicrobials without affecting functionality [13,17–19].

In the present work we studied the interaction of enterocin CRL35 with simplified models mimicking Gram-positive plasma membranes. We intended to describe membrane determinants that affect peptide affinity and the effects of the peptide on membrane properties and structure. Results indicate that peptide readily partitions to bacterial lipid interfaces, but modifies phospholipid membrane properties either increasing and decreasing ordering and hydration depending on the acyl chain length. Importantly, peptide induced bilayer to non-bilayer structural rearrangement of membrane model systems, which correlated with bilayer permeabilization activity. Our results strongly support a two-step mechanism involving the two peptide domains.

## 2. Materials and Methods

### 2.1. Reagents

Lipids 1-palmitoyl-2-oleoyl-*sn*-glycero-3-phosphoethanolamime (POPE), 1,2-dilauroyl-*sn*-glycero-3-phospho-(1'-*rac*-glycerol) sodium salt (DLPG), 1,2-dimiristoyl-*sn*-glycero-3-phospho-(1'-*rac*-glycerol) sodium salt (DMPG) and 1,2-dipalmitoyl-*sn*-glycero-3-phospho-(1'-*rac*-glycerol) sodium salt (DPPG) were purchased in their powder presentation to Avanti Polar Lipids, USA, and used as received. All other chemicals were ACS grade from Sigma. Solvents were HPLC grade from Merck. Buffer solutions were prepared with ultra pure water with 18.2 MΩ.cm resistivity obtained from HealForce Purifier.

Enterocin CRL35 was synthetized by Fmoc chemistry on a Rink amide 4-methylbenzhydrylamine resin and purified by HPLC, as described previously [9].

Lipid solutions were prepared in a chloroform:methanol 2:1 solvent mixture and stored in PTFE (Teflon TM) caped vials at -20 °C until use. Lipid mixtures were prepared dispensing appropriate amounts with glass syringes (Hamilton, NV, USA).

### 2.2. Langmuir monolayers

Monolayer adsorption experiments were carried out in a 7 mL custom made PTFE trough and the surface tension was continuously measured with a Wilhelmy paper plate on a NIMA 102M device, KSV NIMA-Biolin Scientific, Sweden. Surface pressure π was calculated according to:

$\pi = \gamma_0 - \gamma$, where $\gamma_0$ is the surface tension of the clean bare water/air interface and γ is the surface tension of the sample [20,21]. Temperature was controlled in the room and set constant at 24 °C.

Peptide Gibbs isotherm was undertaken for studying surface activity of enterocin CRL35 by injection of small volumes of peptide into 145 mM NaCl subphase with continuous and gentle stirring for ensuring uniform distribution and equilibration at the interface [22]. Surface pressure was determined until equilibrium value was reached, typically 15 minutes.

Peptide affinity toward lipid interfaces was studied calculating the exclusion surface pressure in lipid monolayers set at different initial surface pressure. Aliquots of DLPG:POPE, DMPG:POPE and DPPG:POPE, all at 8:2 mole ratio, were spread in small drops onto 145 mM NaCl subphase until the desired initial value of surface pressure ($\pi_i$ in Figure 3) was reached. Monolayers were set to stand 5 min for solvent evaporation and peptide was injected with a glass Hamilton syringe beneath the monolayer at a final concentration of 150 nM, determined

by the Gibbs isotherm plateau (see below). After peptide injection, the increase in surface pressure (Δπ) produced by peptide penetration in lipid monolayer was calculated when an equilibrium surface pressure ($\pi_{eq}$) was attained, typically at 20 minutes, according to $\Delta\pi=\pi_{eq}-\pi_i$. Exclusion surface pressure was determined as the $\pi_i$ value at which Δπ is null, by extrapolating Δπ up to $\pi_i$ axis intersection [22,23].

Elasticity of lipid films was determined by means of compression isotherms in Langmuir monolayers of the different mixtures. Small aliquots of chloroform lipid solutions were spread onto 145 mM NaCl subphase in a NIMA 102M balance equipped with two Delrin mobile barriers. Monolayers were set to stand during 5 minutes and compressed isometrically at 2 $Å^2$.molec$^{-1}$.s$^{-1}$ up to film collapse. Surface compressibility modulus K was calculated according to: $K = C_S^{-1} = -A\frac{\partial\pi}{\partial A}$, where A is the mean molecular area of the lipid mixture at the surface pressure value of π [20,24].

**2.3. Infrared spectroscopy**

Lipid vesicles were prepared with the same lipid mixtures used in monolayer experiments. Lipid solutions were dried under nitrogen flow and vacuum and hydrated at 15 mM final concentration with 10 mM Hepes buffer containing 100 mM NaCl and 1 mM EDTA, pH 7.4. After vigorous vortexing, multilamellar vesicles were subjected to three freeze-thaw cycles from 45 to -20 °C and sonicated in a bath sonifier during 20 minutes until clarity. Peptide was freeze-dried three times in the presence of 10 mM HCl in order to remove TFA counterion used during peptide synthesis.

Infrared spectroscopy was carried out in a Thermo Nicolet 5700 spectrometer, equipped with DTGS detector and dry air purge (ParkerBalston, MA, USA). Demountable liquid cell with $CaF_2$ windows and 56 µm PTFE spacers (HarrickSci, NY, USA) were used for transmission spectra acquisition, from 4000 to 1100 cm$^{-1}$. Sample cell was thermostated with custom made cell aluminum jacket for water circulation pumped by an external chiller (J.P.-Selecta, BCN, Spain). Temperature was measured directly on cell windows with a custom-made K thermocouple (Arion SA, SMT, Arg). Spectra were acquired averaging 56 spectra at a resolution of 2 cm$^{-1}$. Samples were prepared in deuterated media, measured at different temperatures and buffer subtracted for studying bands of methylene and carbonyl vibrational modes of membrane phospholipids [25,26] and peptide Amide I, which senses protein secondary structure [27,28]. Spectra subtraction and band center of mass were calculated with OMNIC software provided by spectrometer manufacturer. Second derivative, Fourier self-deconvolution of spectra and

fitting procedure for determining the contribution of the components to the overall experimental band was done as described previously [27,29,30].

**2.4. X-ray scattering at synchrotron source**

Small angle X-ray scattering (SAXS) was measured at SAXS1 beamline of UVX synchrotron source of Laboratorio Nacional de Luz Sincrotron (LNLS) – CNPEM, Brazil, which produces 8 KeV photons, wavelength 1.488 Å. A Pilatus 300K area detector, Dectris, Switzerland, located at 1.2 m was used for recording X- ray patterns. Radial integration was carried out with Fit2D scripts [31] adapted by beamline staff. Samples were prepared similarly to FTIR experiments and loaded on a liquid sample holder with mica windows and PTFE spacers, with temperature controlled by an external circulating water bath. Control samples (15 mM lipid final concentration) were first measured in a temperature ramp from 20 to 40 °C; then samples were co-incubated with peptide at 20:1 lipid:peptide mole ratio and measured in the same temperature ramp. Also, buffer (10 mM Hepes, 100 mM NaCl, 1 mM EDTA, pH 7.4) was measured at the same temperatures for subtracting baseline signal to samples.

**2.5. Zeta potential determination**

Liposomes were prepared as for FTIR experiments but a 0.1 mM final concentration and buffer diluted 1:10 in order to reduce counter-ion interference of surface charges. Measurements were undertaken in a Nano-particle analyzer (Horiba SZ100, Japan) at 25 °C. Results are the average of 10 readings of duplicate samples.

**2.6. Membrane permeability assay**

Fluorescent loaded vesicles were prepared for undertaking leakage assay in order to study membrane permeabilization by enterocin CRL35. Lipid vesicles were prepared with the same protocol described above except 30 mM calcein in 10 mM Hepes buffer pH 7.4 was used. Non-entrapped calcein was eliminated by size exclusion chromatography in a Sephadex G75 column, 7x80 mm, equilibrated and eluted with 10 mM Hepes, 100 mM NaCl and 1 mM EDTA, pH 7.4. Liposomes were quantified by measuring phosphate with molibdenum based technique as reported previously [32]. Experiments were carried in quartz cuvettes with liposomes diluted in the same buffer at a lipid final concentration of 20 μM. Fluorescence excitation and emission wavelengths were set at 490 and 518 nm, respectively, with slits of 8 nm full width at half maximum for both channels. Fluorescence data collected in photon counting mode in a SLM 4048c-Phoenix device equipped with Peltier unit for temperature control (ISS, IL, USA). Liposomes were set to stand 10 minutes for checking bilayer stability and

the experiment was initiated by successive additions of the antimicrobial peptide. Emission was recorded continuously, and the experiment ended with addition of Triton X-100 to reach a final concentration of 0.1 % w/v. Permeabilization degree was calculated according to:

$\% = \frac{I-I_0}{I_f-I_0}.100$, where I, $I_0$ and $I_f$ stand for emission intensity of the sample upon addition of peptide, fluorescence intensity of vesicles at the beginning of the experiment and fluorescence measured after the addition of Triton X-100, respectively.

## 3. Results

Peptide structure in solution was studied with infrared spectroscopy, using deuterated media in order to measure Amide I' absorption band, which is sensitive to secondary structure elements. Spectra showed an asymmetric band in the range 1700-1600 $cm^{-1}$ (Figure 1) suggesting that the peptide has a structured backbone even when dissolved in aqueous media.

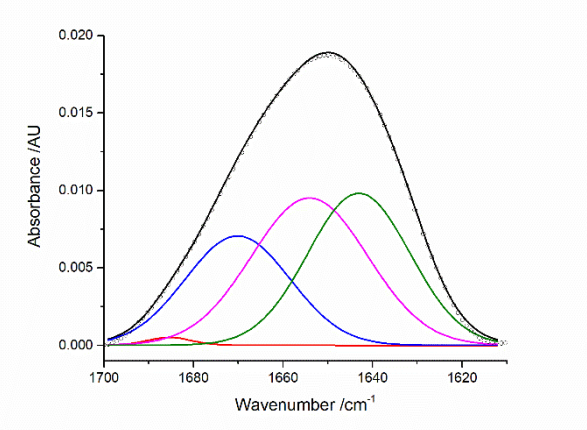


**Figure 1.** Enterocin CRL35 Amide I' absorption band analysis for peptide secondary structure determination. Spectra baseline was corrected by substracting buffer spectrum at the same temperature. Peptide concentration was 470 nM. in buffer prepared in D2O. Spectrum shown (black line) is representative of three independent experiments, taken at 30 °C in 10 mM Hepes, 100 mM NaCl, 1 mM EDTA, pH 7.4 buffer prepared in $D_2O$. Colored lines are the component bands obtained after fitting with the experimental spectrum, as explained in Section 2.3.

Analysis of the Amide I component bands indicated 37% was associated to typical α-helix signals, whereas turns+β structures signals were also present (~28%). On the other hand, only ~30% of the peptide may lack a defined structure (Table 1), which was indeed, an interesting feature if we consider that similar peptides proved to have no structure at all in buffer.

**Table 1.**

| Band ($cm^{-1}$) | % | Secondary structure |
|---|---|---|
| 1685.4 | 0.8 ± 0.4 | β sheet (high freq) |
| 1670.1 | 24.8 ± 2.2 | Turn |
| 1654.1 | 37.2 ± 1.4 | α helix |
| 1643.1 | 33.7 ± 2.6 | Unordered |
| 1632.4 | 3.5 ± 1.0 | β sheet (low freq) |

Component bands of enterocin CRL35 Amide I' band. Area of each component was considered as the relative contribution of each secondary structure element to the overall peptide folding. Results shown are the mean ± standard deviation of three independent experiments.

In order to get insights on the molecular properties and surface activity of enterocin CRL35, we first measured the Gibbs isotherm at air:water interface. The peptide presented interfacial activity when injected into a subphase made of 145 mM NaCl, reducing the surface tension of the water/air interface by 10 $mN.m^{-1}$ at concentrations above 200 nM, as depicted in Figure 2.

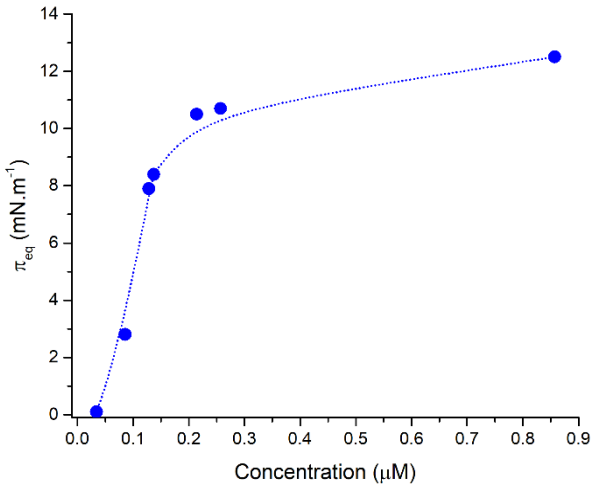


**Figure 2.** Gibbs isotherm of enterocin CRL35 in 145 mM NaCl subphase. The surface pressure at equilibrium was measured after 15 min peptide injection into subphase at the indicated final concentration.

Enterocin CRL35 also readily interacted with lipid monolayers, producing significant reduction of the surface tension (or increase of π) of water/lipid/air interfaces when injected below preformed PG:PE monolayers (Figure 3), even at surface pressure values higher than 10 $mN.m^{-1}$, the equilibrium surface pressure of peptide at 200 nM in the subphase. In order to evaluate the effect of membrane properties on the interaction with peptide, three lipid mixtures were studied by changing the acyl chain length of the PG component whilst keeping constant the PG:PE ratio (8:2). The exclusion surface pressure calculated for enterocin CRL35 interaction with DLPG:POPE, DMPG:POPE and DPPG:POPE monolayers was 29, 25 and 22 $mN.m^{-1}$, respectively, indicating a higher affinity of peptide toward mixtures made of PG species with shorter acyl chains.

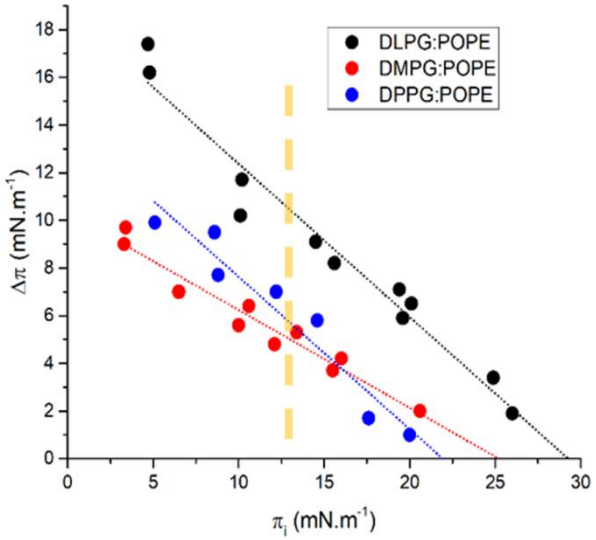


**Figure 3.** Enterocin CRL35 interaction with PG:PE monolayers at 8:2 mole ratio. Increase of the surface pressure (Δπ) due to peptide penetration in monolayers set at different initial surface pressures ($\pi_i$) was measured after peptide injection beneath the lipids at a final concentration in the subphase of 150 nM. Dotted lines are the linear regression of the experimental points (solid circles); dashed vertical line depicts equilibrium surface pressure of the peptide in bare air/water interface at the assayed concentration.

This result was counterintuitive, as enterocin has been reported to show higher affinity toward ordered membranes [33], the latter being related to membrane lipids with long hydrocarbon chains. However, when we determined the surface compressibility modulus of the lipid mixtures, we found that PG with shorter acyl chain, DLPG, formed stiffer monolayers when mixed with POPE compared to DMPG and DPPG, as shown in Figure 4. DMPG:POPE mixture showed the lowest value of K at 30 mN.m$^{-1}$, which may explain the lowest increment in surface pressures upon peptide injection. However, exclusion surface pressure of enterocin CRL35 was slightly higher in DMPG:POPE than in DPPG:POPE.

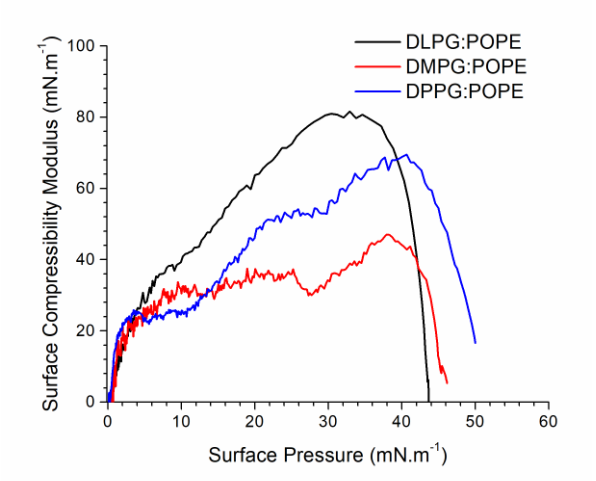

**Figure 4.** Surface elasticity of PG:PE monolayers at 8:2 mole ratio. The surface compressibility modulus was calculated as indicated in Section 2 from the compression isotherms made at 24 °C. Results shown are representative of two independents experiments.

This finding is not unexpected since PG and PE were previously reported to interact favorably [34]. Also, the components of DLPG:POPE present the most similar transition surface pressures of the assayed mixtures, leading to a mixed film with most favorable interactions between components.

In order to study the bacterial membrane-peptide interaction in bilayers, sonicated vesicles were prepared with the same lipid mixtures used for monolayer experiments. Samples were first analyzed with infrared spectroscopy in order to get insights on both membrane and peptide dynamics at molecular level. Ordering of the acyl chains was evaluated with the methylene vibrational modes, measuring the dependence with temperature of the band center of mass circa 2850 $cm^{-1}$. This band corresponds to the symmetrical stretching vibrational mode ($v_s$) of methylene groups and it 'is sensitive to the number of gauche/trans conformers in acyl chains [25]. The short chain PG variant, DLPG, mixed with POPE formed liquid crystalline liposomes as indicated by the high wavenumber values of $v_s$ $CH_2$ in the entire range of temperatures (Figure 5a), whilst DMPG and DPPG mixtures presented a single transition temperature (Figure 5b and 5c, respectively), indicating complete mixing of PG and PE components. Enterocin CRL35 exerted a dual effect on membranes when incubated with liposomes made of PE and PG, depending on the acyl chain length. On the one hand, the order degree of DLPG:POPE liposomes was lowered upon addition of the bacteriocin as indicated by the increase in $v_s$ $CH_2$ wavenumbers (Figure 5a, red circles). On the other, DMPG:POPE liposomes were almost unaffected, except for a small ordering of acyl chains (Figure 5b). Finally, DPPG:POPE liposomes showed no change in the wavenumbers but a significant shift to higher values of the transition temperature (Figure 5c), indicating a gel phase stabilization by the peptide.

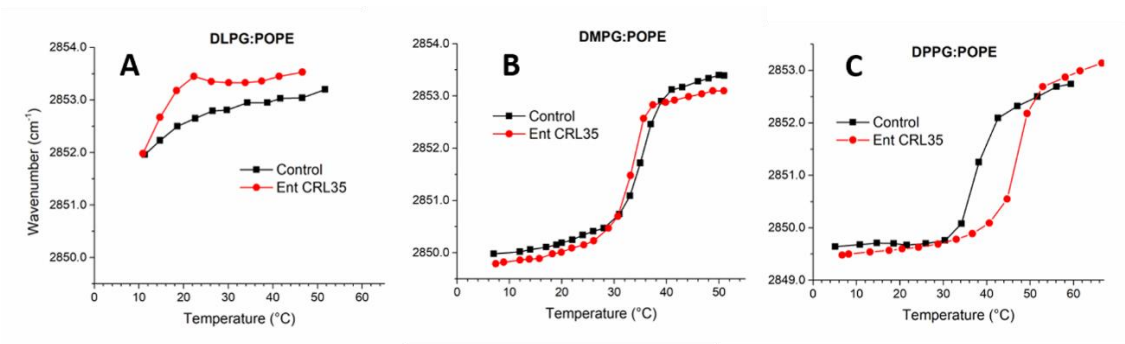

**Figure 5.** Enterocin CRL35 interaction with PG:PE liposomes prepared at 8:2 mole ratio in 10 mM Hepes, 100 mM NaCl, 1 mM EDTA, pH 7.4 in $D_2O$. Evolution of the $\nu_s$ vibrational mode of methylene groups with temperature of liposomes at a lipid concentration of 15 mM in the absence and presence of peptide, 20:1 lipid to peptide mole ratio. Results shown are representative of three independent experiments.

Interfacial region of the membrane was studied by infrared spectroscopy by analyzing stretching vibrational mode of carbonyl groups ($\nu_{CO}$) of glycerophospholipids at 30 °C. The absorption band at 1770-1700 $cm^{-1}$ spectral region is asymmetric due to the contribution of both hydrogen and non-hydrogen bonded carbonyl groups with water at 1725 and 1742 $cm^{-1}$, respectively [35]. The components bands were calculated and the contribution of each group to the overall band was considered equal to the relative amount of hydrogen and non-hydrogen bonded carbonyl groups.

DLPG:POPE liposomes presented a higher contribution of the low frequency band corresponding to hydrated carbonyls compared to DMPG and DPPG mixtures (Table 2). As expected, the mixture was at liquid crystalline phase at the working temperature (30 °C). When the liposomes were co-incubated with the peptide, a small overlap of the bands of $\nu_{CO}$ and Amide I' vibrational modes was observed. This overlap is due to the low frequency and low intensity band of PE carbonyl groups [36] and the high frequency and low intensity of some amino acid lateral chains [27,28]. Thus, both carbonyl and backbone bands were treated and fitted simultaneously, as can be observed in Figure 6. Hydration level of the membrane interfacial region was not affected by enterocin CRL35 when co-incubated with of DLPG:POPE liposomes (Table 2), whereas it was increased it in the case of DMPG:POPE ones. On the other hand, interfacial region of DPPG:POPE liposomes showed an increase of dehydrated carbonyl groups upon peptide interaction (Table 2).

**Table 2.**

| Sample | Band ($cm^{-1}$) | Control (%) | Ent (%) |
|---|---|---|---|
| DLPG:POPE | 1742.8 | 40.0 ± 2.1 | 42.1 ± 1.8 |
| | 1725.7 | 50.1 ± 1.9 | 51.6 ± 1.6 |
| | 1707.5 | 9.9 ± 2.9 | 6.3 ± 3.0 |
| DMPG:POPE | 1740.9 | 46.2 ± 1.8 | 36.8 ± 1.9 |
| | 1722.9 | 42.4 ± 2.0 | 51.5 ± 1.7 |
| | 1705.0 | 11.4 ± 3.0 | 11.7 ± 2.8 |
| DPPG:POPE | 1741.2 | 56.6 ± 1.9 | 63.0 ± 1.5 |

| | | | |
|---|---|---|---|
| | 1724.2 | 40.1 ± 2.1 | 32.5 ± 1.6 |
| | 1706.5 | 3.3 ± 1.8 | 4.5 ± 2.2 |

Analysis of the component bands of ν vibrational mode of carbonyl groups of PG:PE 8:2 mole ratio liposomes at 30 °C in the absence (control) and presence of enterocin CRL35 (Ent). Relative area of the components normalized to the total area of the experimental band are shown in %. The band circa 1742 $cm^{-1}$ corresponds to carbonyl groups that are not hydrogen bonded to water, whereas band circa 1724 $cm^{-1}$ corresponds to carbonyl groups hydrogen bonded to water.

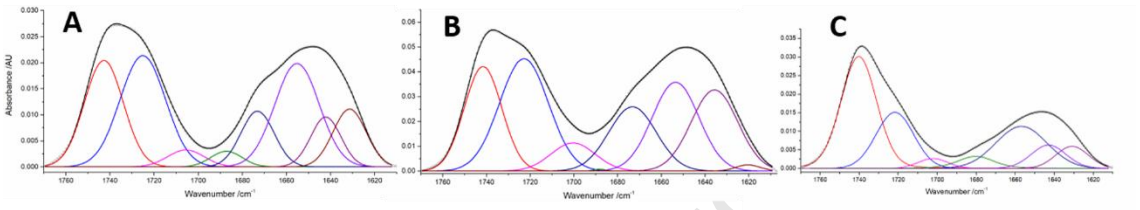


**Figure 6.** Analysis of ν of carbonyl groups and Amide I' vibrational modes of PG:PE mixtures of 8:2 mole ratio and enterocin CRL35, respectively, in order to get hydration level of membrane and peptide secondary structure at 30 °C. Liposomes of DPPG:POPE (A), DMPG:POPE (B) and DLPG:POPE (C) at 15 mM final concentration were co-incubated with the bacteriocin at 20:1 lipid:peptide mole ratio. Spectra shown (black lines) are representative of three independent experiments. Colored lines are components bands obtained after fitting with experimental spectrum as explained in Section 2.3.

In order to evaluate peptide secondary structure upon membrane interaction, the asymmetric band of the Amide I vibrational mode was analyzed for retrieving component bands of the corresponding secondary structural elements (Figure 6). As it can be observed in Table 3, the main structural rearrangements for the three membrane models assessed consisted of an increase of β sheet with a concomitant reduction of the unordered component. Even more, in the presence of DPPG:POPE liposomes, the α-helix component also increased.

**Table 3.**

| DLPG:POPE_ent | | DMPG:POPE_ent | | DPPG:POPE_ent | | |
|---|---|---|---|---|---|---|
| Band ($cm^{-1}$) | % | Band ($cm^{-1}$) | % | Band ($cm^{-1}$) | % | Secondary Structure |
| 1687.2 | 4.7 ± 2.1 | 1688.2 | 0.2 ± 0.1 | 1680.2 | 11.7 ± 1.3 | β sheet (high freq) |
| 1673.1 | 17.9 ± 1.9 | 1673.2 | 27.4 ± 1.4 | | | Turn |
| 1655.2 | 44.3 ± 1.8 | 1653.5 | 37.2 ± 1.4 | 1656.8 | 51.5 ± 1.2 | α helix |
| 1642.1 | 14.6 ± 2.1 | | | 1642.8 | 19.7 ± 1.6 | Unordered |
| 1631.4 | 18.4 ± 1.4 | 1635.7 | 33.8 ± 1.3 | 1630.8 | 17.1 ± 1.2 | β sheet (low |

| | | | | | | |
|---|---|---|---|---|---|---|
| | | | | | | freq) |

Component bands of enterocin CRL35 Amide I' band upon interaction with PG:PE 8:2 mole ratio liposomes. Area of each component was considered as the relative contribution of each secondary structure element. Results shown are average of three independent experiments.

Membrane structure was also evaluated by means of X- ray scattering at small angle in liposome dispersions co-incubated with enterocin CRL35 at different temperatures. Figure 7 depicts that control samples had no sharp Braggs peaks but the signal was dominated by the form factor of uncorrelated vesicles, due to Coulombic repulsion forces of PG component. Although signal to noise ratio was not high enough for obtaining reliable structural modeling of the membrane electron density profiles, the second minimum of scattering patterns suggests thicker bilayers [37] for DPPG:POPE liposomes (minima at lower q values) compared to DMPG:POPE and DLPG:POPE, as predicted. Also, on top of the broad Bragg scattering, peaks at 0.75 and 1.5 $nm^{-1}$ can be observed for DLPG:POPE mixtures, produced by a small population of correlated vesicles with periodicity of 8 nm. In the case of DPPG:POPE, two peaks over the Bragg signal are present at 1 and 1.5 $nm^{-1}$, which correspond to a periodicity of 6 nm. However, they probably represent the second and third order, being the first order peak at the form factor minimum at 0.5 $nm^{-1}$, which indicates a periodicity of 12 nm.

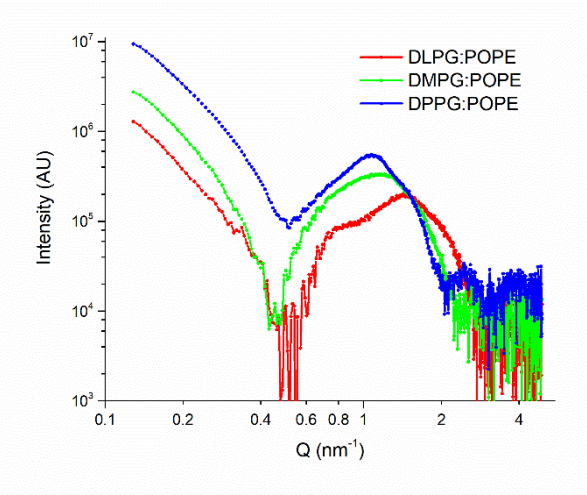


**Figure 7.** Synchrotron X- ray scattering of PG:PE 8:2 mole ratio liposomes measured at 20 °C. Samples were prepared at lipid final concentration of 15 mM.

Membrane X-ray scattering changed dramatically when vesicles were incubated with enterocin CRL35. The positively charged peptide prevented electrostatic repulsion between vesicles, and Braggs peaks from correlated systems could be measured in the different systems (Figure 8). Moreover, the X-ray scattering patterns indicated mesomorphic rearrangement of membranes

from bilayer to non-bilayer structures. In the case of DLPG:POPE vesicles, the addition of peptide induced a pattern with two main peaks in 1 to 2 ratio, which suggests lamellar array with D spacing of 2π/Q of 8.22 nm at 20 °C (Figure 8a). Also, a poorly resolved peak could be inferred located at √2 of the first order main peak (Figure 8a), suggesting that a cubic phase was coexisting with lamellar bilayers. On the other hand, DMPG:POPE and DPPG:POPE vesicles co-incubated with enterocin CRL35 presented lamellar like X-ray patterns, mainly, at 20 °C and with D spacing of 8.49 and 8.85 nm, respectively (Figures 8b and c). The latter increment on thickness is consistent with the contribution of 0.126 nm per methylene group in trans configuration [38] in palmitoyl chains compared to myristoyl ones, and considering that PG component was only 80% of the total lipid mixture. Thus, two methylene groups per monolayer would add ~0.5x0.8 = 0.4 nm when comparing DPPG:POPE and DMPG:POPE. However, the thickness increment of DMPG:POPE compared to DLPG:POPE is smaller than predicted, which is probably a consequence of the dual effect of enterocin CRL35 on the different phospholipid mixtures depending on the PG acyl chain length: disordering on DLPG:POPE and ordering on DPPG:POPE.

At increasing temperatures, peaks with q spacing of non-bilayer structures occurred with higher intensity, suggesting co-existence of lamellar with cubic, in the case of DMPG:POPE-enterocin (Figure 8b), and lamellar with hexagonal II, in the case of DPPG:POPE-enterocin (Figure 8c). At 40 °C, the mixture DMPG:POPE incubated with peptide presented an X-ray pattern of pure cubic phase (Figure 8b).

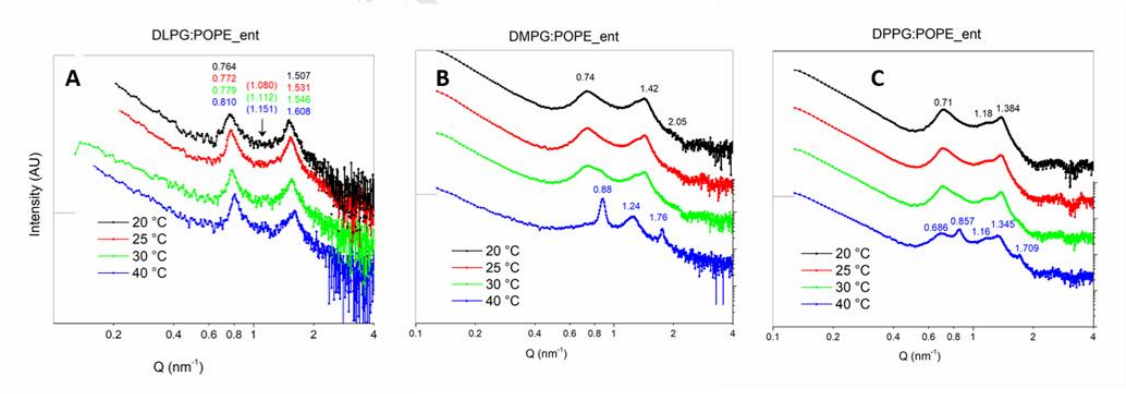


**Figure 8.** Synchrotron X-ray scattering of liposomes made of PG:PE 8:2 mole ratio in the presence of enterocin CRL35 at 20:1 lipid:peptide mole ratio measured at different temperatures. Lipid concentration: 15 μM.

The overall charge of the different PG:PE vesicles in the presence of enterocin CRL35 was estimated by zeta potential measurements. Results shown in Table 4 indicate negatively

charged liposomes, as expected due to the high content of PG. Interestingly, the peptide reduced the negative potential of DLPG:POPE and DPPG:POPE vesicles, but in the conditions studied induced negligible neutralization of DMPG:POPE system.

**Table 4.**

| | Zeta potential (mV) | | |
|---|---|---|---|
| Lipid:peptide mole ratio | DLPG:POPE | DMPG:POPE | DPPG:POPE |
| 0 | -136.3 ± 3.8 | -75.3 ± 4.3 | -99.3 ± 3.1 |
| 20:1 | -100.6 ± 5.8 | -83.5 ± 3.7 | -92.6 ± 2.5 |
| 10:1 | -39.3 ± 6.1 | -71 ± 5 | -39.6 ± 1.4 |

Zeta potential of liposomes made of PG:PE at mole ratio 8:2 in the absence and in the presence of enterocin CRL35. Lipid final concentration was 0.1 mM, temperature 25 °C. Measurements were read 10 times in duplicate samples. A low ionic strength buffer was used: 1 mM Hepes, 10 mM NaCl, pH 7.4.

Functionality of enterocin CRL35 was assayed in terms of its capability of perturbing bilayer permeability on calcein-loaded liposomes. Experiments at two peptide concentrations indicated that liquid-crystalline DLPG:POPE liposomes were permeabilized up to 50% at an optimal temperature of 30 °C (Figure 9a). However, liposomes prepared with DMPG:POPE and DPPG:POPE were permeabilized only at 20 and 30 °C (Figures 9b and c, respectively), below the transition temperature of both systems.

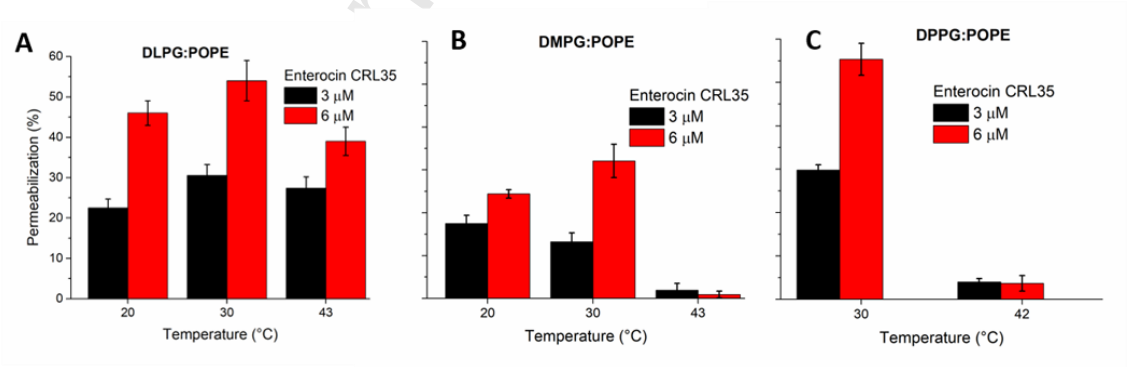


**Figure 9.** Permeabilization of calcein-loaded liposomes by enterocin CRL35. Three PG:PE lipid mixtures were assayed at different temperatures and permeabilization calculated as indicated in Section 2.6.

## 4. Discussion

Self-assembly of biomolecules plays an utmost important role in cellular structures, such as biomembranes, proteinaceous pores, amyloid aggregation, as well as in biotechnological applications. Membrane structure and peptide supramolecular assemblies have been thoroughly studied the last years partly due to their putative roles in the mechanism of action of antimicrobial peptides and the necessity of novel antimicrobial therapies. A major step of this mechanism of action relies on the modification of bilayer properties of biomembranes, especially selective permeability [12,13,17]. Peptides ability to bind and interact with membranes depends on their physicochemical properties that in turn regulate their final interfacial activity [17,39]. Enterocin CRL35 possess both amphipatic sequence and folding as well, in which the hydrophobic C-terminal has a propensity of form an α-helix and the N-terminal contains four lysine residues that may fold in a β structure. Indeed, enterocin decreases the surface tension of water/air interface by 13 $mN.m^{-1}$. Although the latter value is comparable to other membrane active peptides [40–43], it is reached at concentrations as low as 200 nM.

PG:PE binary mixtures have been previously used as bacterial membrane mimics, mainly focused on Gram-negative cells [44–49]. Although this is a rather simplified model that does not take into account compositional molecular diversity of biological membranes, we make use of it for pointing out the main characteristics of Gram-positive bacterial membranes: the presence of negatively charged lipids such as PG in high amounts compared to zwitterionic lipids; and phospholipids with small headgroups such as PE [50,51], which confer negative curvature to membrane interfaces. In the case of *L. monocytogenes*, the target bacterium for enterocin CRL35, plasma membrane is composed by PG, cardiolipin and lysyl-derivatives of both [50,52,53]. Cardiolipin is also a negatively charged phospholipid synthetized by the condensation of two PGs [54]. The final molecular structure consists in two phophatidic acids joined by a glycerol residue; hence, it has four acyl chains per molecule. However, polar head group of cardiolipin is small compared to the volume of the fatty acids, being part of the lipids that introduce negative curvature to interfaces due to their coned molecular shape [55,56]. Actually, cardiolipin can form hexagonal HII phase in the presence of divalent cations [57]. On the other hand, attachment of lysine residues to polar head groups of lipids is a typical modification of Gram-positive bacteria [58] that changes the net charge of PG and cardiolipin from negative to positive partially masking the anionic nature of bacterial membranes [59,60]. Thus, we decided to include a 20 % of PE, as a lipid with small polar head and no net

charge. The other component was PG and taking into account that it shares the chemical groups of the polar head with cardiolipin, the latter was not included. Besides, we could not have a reliable source of cardiolipin that provides molecular variants. On top of that, the use of only two phospholipids allowed us to keep the system as simple as possible. We also varied the acyl chain length of PG species for modifying mechanical properties of membrane model systems, considering the apparent dependence of enterocin CRL35 biological activity on cell membrane ordering [33]. It' has been demonstrated in a combined study of diffuse X-ray scattering and neutron diffraction of phosphatidylglycerol bilayers that lengthening of the hydrocarbon chains renders membranes stiffer, with higher bending modulus, due to the decrease in lateral area that leads to stronger van der Waals forces in the membranes hydrophobic region [61].

The binary lipid mixture was used for assessing enterocin CRL35 interaction with bacterial membranes. In the presence of DLPG:POPE lipid monolayers, enterocin CRL35 could reach higher surface pressures, up to 32 $mN.m^{-1}$, which represents more than twice that peptide in bare air/water interface, indicating that enterocin would spontaneously insert in bacterial membranes with high content in PG [64]. Moreover, the significance of this result is in line with the concentration used in the experiments, *i.e.* 150 nM, which is in the range of the minimal inhibitory concentration of the bactericidal activity of enterocin CRL35 [62].

In mixtures made with PG with longer acyl chain length, DPPG:POPE and DMPG:POPE, exclusion surface pressure was lower, which was, in principle, against previous evidence that suggested that enterocin preferred ordered membranes in cells [33]. However, surface compressibility modulus indicated that DLPG:POPE monolayers were stiffer than those made with DMPG and DPPG, thus results from model membrane and *in vivo* systems agree after all. Favorable interactions between PE and PG species have been described in the literature, specially between phospholipids acylated with saturated fatty acids [34,44,45,48]. Also, transition surface pressure is an important determinant for predicting mixing of different components, as observed for example in ceramide-sphingomyelin mixed monolayers, in which sphingolipids with highly dissimilar acyl chain lengths mixed favorably provided they shared a similar transition surface pressure [63]. Our results in PG:PE mixed monolayers also indicate that the stiffest PG:PE film is not the one with the longer and more similar acyl chains, DPPG:POPE, but instead DLPG:POPE. This is a consequence of strong molecular interactions between these two phospholipids, which have the closest transition surface pressure values.

In a previous study of binary PG:PE mixtures in bilayers, lipids acylated with saturated fatty acids showed complete mixing when the difference between main transition temperatures was lower than 20 °C [34]. Although mixtures displayed broad endotherms, peaks of pure components that would indicate segregation of some of the components were not observed. Our infrared spectroscopy results also indicate complete mixing of PG and PE components in the different mixtures assayed in bilayer model systems, as a single ordered-disordered transition could be measured with the vibrational mode $\nu_s$ of methylene groups and at temperatures intermediate between pure components.

Interestingly, the peptide effect on liposomes depended on the PG acyl chain length. At the hydrophobic region, the peptide decreased the order of the acyl chains of the thinnest and most disordered lipid mixture, DLPG:POPE, whereas the amount of hydrogen-bonded carbonyl groups was not affected. On the other hand, enterocin CRL35 increased transition temperature of the thicker and more ordered membrane, DPPG:POPE and also the amount of de-hydrated carbonyl groups.

The impact on the hydrophobic region rather than on the interfacial region in DLPG:POPE mixtures can lead to lateral pressure disbalance, inducing lipid phases with inverted curvature[65]. However, interaction of enterocin at polar/interfacial level of membrane cannot be ruled out. PG imparts negative charge to vesicles, which produces coloumbic repulsion between vesicles, as clearly observed by the X-rays diffuse scattering. The latter pattern dramatically changed in the presence of the peptide showing correlated diffraction Bragg peaks that indicate partially screening of liposomes negative charges. Similarly to enterocin CRL35 effect, a synthetic designed amphiphilic peptide composed of multiple alanine residues and a terminal arginine also induced changes in X-pattern of POPG:POPE 2:8 vesicles from form factor lobes to Bragg peaks [66], which was interpreted by the authors as screening of the negative charge of liposome by a surface location of peptide. Evidence of electrostatic interaction of enterocin CRL35 with model membranes is also supported by the increase in zeta potential of liposomes co-incubated with the peptide. Relevance of anionic lipids on bacteriocin activity is also observed in cells, where resistance of some Gram -positive bacteria to antimicrobial peptides is related to the increase of PG modified with lysyl groups by means of the activity of MprF protein [67].

In the case of DPPG:POPE samples, infrared spectroscopy demonstrated gel phase stabilization, which favors flat bilayer and dehydration of the interfacial region. This finding strongly suggests that peptide locates mainly at this region, partly screening negative

charges of PG. The latter was confirmed by SAXS, but in this case cubic and HII phases were formed only when temperature was raised, indicating that acyl chains disordering is also necessary for achieving negative curvature of the membrane interface by increasing lateral pressure because of the membrane hydrophobic region.

An unexpected result was the finding that there were no membrane permeabilization by the peptide in DMPG:POPE and DPPG:POPE mixtures at higher temperatures, in spite of the induction of pure cubic phase. Interestingly, enterocin CRL35 did induce a significant permeabilization and membrane phase coexistence between lamellar and inverted curvature states at lower temperatures for these mixtures. Thus, lamellar to cubic mesomorfism led by enterocin CRL35 when temperature increased occurred through a non-leaky mechanism. Taking into account that this peptide induced vesicle apposition, as indicated by appearance of Braggs peaks in the X-ray patterns, phase transition may occur through a cooperative fusion at vesicle contact points. On the other hand, the stronger permeabilizaton effect of the peptide on DPPG:POPE liposomes in the gel phase is in line with its known preference with ordered membranes, as discussed above. Even though the biological relevance of gel phase was traditionally underrated, increasing evidence indicate that even bacterial membranes can present ordered-disordered phase coexistence [49,68,69] and also ternary lipid mixtures can form gel phases [70] like single lipids at specific temperatures. Attempts to measure order parameters by means of electron paramagnetic resonance [71] and fluorescence anisotropy in whole cells [33,72] suggest that *Listeria* membrane is actually more ordered than typical fluid phases of single lipids and multiple domains may be present. In addition, enterocin-sensitive cells present higher values of DPH fluorescence anisotropy than resistant ones [33]. It must also be taken into account that homeoviscous adaptation of membranes is an important mechanism for survival of bacterial cells at different temperatures, specially in the case of *Listeria*, a bacteria that is able to grow and contaminate food at low temperature, although membrane fluidity is regulated mainly by incorporation of fatty acids with branched chains [72,73].

The dependence of both the temperature phase transition and the dimensions of the cubic phase with the liposome composition in bacterial lipid-enterocin CRL35 systems indicates that membrane permeabilization does not proceed by a peptide-only pore, such as the barrel stave model, but a lipid-peptide structure as proposed in the toroidal pore model [18]. The latter mechanism also agrees with our studies on enterocin CRL35-bacterial model membranes interaction because negative curvature of the lipid interface at local

points on the surface is needed for toroid formation. However, loss of the selective barrier properties of membrane can be produced by means of either discrete toroidal pore structures or perturbance of lipid dynamics on bilayer.

Negatively charged lipids are known to stabilize and favor flat bilayers and/or direct micelles (positive curvature) [74] instead of negatively curved lipid structures. Thus, charge screening is necessary though not enough for having non-zero curved interfaces, as discussed above. Also, it has previously been reported that PEs with longer acyl chains present lower temperature of lamellar to inverted lipid phase transition (Lα to HII) [75], because long chains introduce higher lateral pressure in the hydrophobic core of membranes than short chains. Our results are also in this trend, *i.e.*, cubic phase is more easily formed when order degree of acyl chains is decreased like in the case of the interaction of enterocin CRL35 with DLPG:POPE, as compared to DMPG:POPE and DPPG:POPE. The antibiotic peptide is acting at the surface level of bilayers by screening the negative charge and also perturbing the hydrophobic core of membranes. Non-lamellar lipid phases induced by peptide interaction has been postulated previously as possible antimicrobial mechanism of action of peptides [76]. However, heating well above bacterial lipid physiological temperatures [77] or using model non-bilayer forming lipids, such as DEPE [78], were necessary to prove the effect. In our hands, the coexistence of bilayer with non-bilayer phases and a corresponding membrane permeabilization were obtained at physiological temperatures.

Previous studies demonstrated that shorter peptides derived from enterocin CRL35 retain activity and some of the properties of the native 43 residues long sequence [6,9]. Half of the peptide, the amino terminal part, concentrates 4 of the 5 lysine residues, plus an aspartate. The sequence homology predicts β-type folding; whereas the carboxy terminal part is mostly hydrophobic and putatively α-helical folded. Our infrared spectroscopy analysis of enterocin CRL35 Amide I' band indicates that peptide in solution has significant amount of secondary structure, mainly α-helix and turns, but also unordered folding. Many antimicrobial peptides are reported to be completely unfolded in solution but, at variance with enterocin CRL35, they are typically shorter than 20 residues and lack functional domains [79–81]. It seems that in solution, the hydrophobic C- terminal of the peptide is already folded as α-helix, whereas the basic N terminal is mainly unordered, although structure in solution of other IIa bacteriocins resolved by NMR indicate they are also unordered [82,83].

The two halves of the peptide can then be conceived as two functional domains, in which the positively charged N-terminal firstly screen the negative charge of PG upon peptide first encounter with bacterial membranes. Supporting this hypothesis, infrared spectroscopy indicates that enterocin CRL35 gains beta structure upon interaction with membranes, allowing this extended configuration an optimal neutralization of the membrane charges. Thus, repulsion between the four positive charges located altogether at the N-terminal favor unordered structure of the peptide in solution; whereas negative charges of membranes screen peptide positive charges upon membrane interaction, leading to backbone folding into beta secondary structure. Other bacteriocins of class II like bactofencin A [84] and mesentericin Y105 [85] also interact with membranes by means of their basic N-terminal, which is folded in beta sheet structure; whereas the hydrophobic C-terminal is related to the final antimicrobial activity. In the case of enterocin CRL35, we postulate that the hydrophobic C-terminal α helix would insert into membrane hydrophobic core, leading to an increase of the internal lateral pressure at acyl chains and a disbalance of the overall pressure profile of the bilayer [86]. Thus, together with the reduction of negative charge repulsion of the anionic phospholipids due to peptide positive charges, negative curvature to the lipid interface can be promoted [55,87,88]. Even though results obtained with model systems cannot be directly extrapolated to *in vivo* systems due to their compositional simplicity and a complete cubic phase transformation of cell membranes is highly unlikely, this work clearly presents intrinsic properties of enterocin CRL35 as a bacterial bilayer disruptor by means of negative curvature induction in negatively charged membranes containing PG and PE.

Modular design and functionality of bacteriocins have been previously postulated for explaining the interaction of the peptides with a membrane receptor and putative pore formation, which would be carried out by N-terminal and C-terminal, respectively [5,89,90]. This model agrees with the present results in a two-step mechanism, where the process is undertaken sequentially by the peptide halves: a first step of binding/recognition by the N-terminal half and then membrane perturbation the by C-terminal domain.

## 5. Conclusions

The bacteriocin enterocin CRL35 interacted with PG:PE 8:2 lipid models intended to mimic Gram positive bacterial membrane, affecting bilayer permeability and inducing non-bilayer lipid structures. The membrane lipid ordering and acyl chain length regulated peptide effect and the temperature threshold for the bilayer-non bilayer coexistence; the latter correlated with peptide-induced membrane permeabilization. Membrane interaction would proceed through a two-step process undertaken by the two halves of the peptide: partition or surface binding to negatively charged membranes involving the basic N-terminal and membrane hydrophobic core perturbation by the insertion of the C-terminal hydrophobic α helix. Screening of membrane surface negative charges and disbalance of the lateral pressure profile both induced by peptide would lead to non-bilayer membrane structural rearrangement.

**Acknowledgments**

Funding was provided by Agencia Nacional de Promoción Científica y Tecnológica ANPCyT, grants PICT 2014 N° 3563 and PICT 2016 0819, FONCYT. SAXS data were collected at LNLS-CNPeM, SAXS1 beamline, Project 20170143, with the collaboration of Antonio Gasperini Malfatti. We thank technical assistance of Mr Rafael Gutiérrez, CCT CONICET Tucumán, for maintenance and operation of infrared equipment and PhD Soledad Bazán, CIQUIBIC CONICET - Universidad Nacional de Córdoba, for assistance in zeta potential measurements. CMA was granted with CIN fellowship, EVC program. CJM, RGO and FGD are researchers of CONICET.

**References**

[1] P.D. Cotter, R.P. Ross, C. Hill, Bacteriocins-a viable alternative to antibiotics?, Nat. Rev. Microbiol., (2013).

[2] J. Nissen-Meyer, P. Rogne, C. Oppegard, H. Haugen, P. Kristiansen, Structure-Function Relationships of the Non-Lanthionine-Containing Peptide (class II) Bacteriocins Produced by Gram-Positive Bacteria, Curr. Pharm. Biotechnol., (2009).

[3] R.E. Hancock, D.S. Chapple, Peptide antibiotics, Antimicrob Agents Chemother, 43 (1999) 1317–1323.

[4] R.E.W. Hancock, H.G. Sahl, Antimicrobial and host-defense peptides as new anti-infective therapeutic strategies, Nat. Biotechnol., (2006).

[5] N.S. Ríos Colombo, M.C. Chalón, S.A. Navarro, A. Bellomio, Pediocin-like bacteriocins: new perspectives on mechanism of action and immunity, Curr. Genet., (2018).

[6] L. Saavedra, C. Minahk, A.P. de Ruiz Holgado, F. Sesma, Enhancement of the enterocin CRL35 activity by a synthetic peptide derived from the NH2-terminal sequence, Antimicrob Agents Chemother, 48 (2004) 2778–2781.

[7] C.J. Minahk, M.E. Farías, F. Sesma, R.D. Morero, Effect of Enterocin CRL35 on Listeria monocytogenes cell membrane, FEMS Microbiol. Lett., 192 (2000) 79–83.

[8] G.S. De Giori, G.F. De Valdéz, A.P. De Ruiz Holgado, G. Oliver, Microflora of Tafí Cheese: Changes During Manufacture and Maturation, J. Food Prot., (1983).

[9] E. Masias, P.R.S. Sanches, F.G. Dupuy, L. Acuña, A. Bellomio, E. Cilli, L. Saavedra, C. Minahk, 28-mer fragment derived from enterocin CRL35 displays an unexpected bactericidal effect on listeria cells, Protein Pept. Lett., 22 (2015) 482–488.

[10]D.E. Barraza, N.S. Ríos Colombo, A.E. Galván, L. Acuña, C.J. Minahk, A. Bellomio, M.C. Chalón, New insights into enterocin CRL35: Mechanism of action and immunity revealed by heterologous expression in Escherichia coli, Mol. Microbiol., (2017).

[11]M. Kjos, I.F. Nes, D.B. Diep, Class II one-peptide bacteriocins target a phylogenetically defined subgroup of mannose phosphotransferase systems on sensitive cells, Microbiology, (2009).

[12]M.R. Yeaman, N.Y. Yount, Mechanisms of antimicrobial peptide action and resistance, Pharmacol Rev, 55 (2003) 27–55.

[13]R.M. Epand, C. Walker, R.F. Epand, N.A. Magarvey, Molecular mechanisms of membrane targeting antibiotics, Biochim. Biophys. Acta - Biomembr., (2016).

[14]S. Qian, C. Wang, L. Yang, H.W. Huang, Structure of the alamethicin pore reconstructed by x-ray diffraction analysis, Biophys. J., (2008).

[15]L. Yang, T.A. Harroun, T.M. Weiss, L. Ding, H.W. Huang, Barrel-stave model or toroidal model? A case study on melittin pores, Biophys. J., (2001).

[16]D. Allende, S.A. Simon, T.J. McIntosh, Melittin-induced bilayer leakage depends on lipid material properties: Evidence for toroidal pores, Biophys. J., (2005).

[17]W.C. Wimley, Describing the mechanism of antimicrobial peptide action with the interfacial activity model, ACS Chem Biol, 5 (2010) 905–917.

[18]Y. Shai, Mode of action of membrane active antimicrobial peptides, Biopolym. - Pept. Sci. Sect., (2002).

[19]M.P. Mingeot-Leclercq, J.L. Décout, Bacterial lipid membranes as promising targets to fight antimicrobial resistance, molecular foundations and illustration through the renewal of aminoglycoside antibiotics and emergence of amphiphilic aminoglycosides, Medchemcomm, (2016).

[20]G. Gaines, Insoluble Monolayers at Liquid-Gas Interfaces, Interscience Publishers, New York, 1966.

[21]P. Dynarowicz-Latka, A. Dhanabalan, O.N. Oliveira Jr., Modern physicochemical research on Langmuir monolayers, Adv Colloid Interface Sci, 91 (2001) 221–293.

[22]R. Maget-Dana, The monolayer technique: A potent tool for studying the interfacial properties of antimicrobial and membrane-lytic peptides and their interactions with lipid membranes, Biochim. Biophys. Acta - Biomembr., (1999).

[23]S.R. Dennison, F. Harris, D.A. Phoenix, Chapter Three - Langmuir-Blodgett Approach to Investigate Antimicrobial Peptide-Membrane Interactions, in: Adv. Planar Lipid Bilayers Liposomes, Academic Press, 2014: pp. 83–110.

[24]S. Ali, J.M. Smaby, H.L. Brockman, R.E. Brown, Cholesterol's interfacial interactions with galactosylceramides, Biochemistry, 33 (1994) 2900–2906.

[25]R.N. Lewis, R.N. McElhaney, Membrane lipid phase transitions and phase organization studied by Fourier transform infrared spectroscopy, Biochim Biophys Acta, 1828 (2013) 2347–2358.

[26]J.L. Arrondo, F.M. Goni, Infrared studies of protein-induced perturbation of lipids in lipoproteins and membranes, Chem Phys Lipids, 96 (1998) 53–68.

[27]J.L.R. Arrondo, A. Muga, J. Castresana, F.M. Goñi, Quantitative studies of the structure of proteins in solution by fourier-transform infrared spectroscopy, Prog. Biophys. Mol. Biol., (1993).

[28]E. Goormaghtigh, V. Cabiaux, J.-M. Ruysschaert, J.R. Harris, Determination of Soluble and Membrane Protein Structure by Fourier Transform Infrared Spectroscopy, in: H.J. Hilderson, G.B. Ralston (Eds.), Physicochem. Methods Study Biomembr., Springer Science, Business Media, New York, 1994: pp. 329–362.

[29]J.A. Fernández-Higuero, A.M. Salvador, C. Martín, J.C.G. Milicua, J.L.R. Arrondo, Human LDL structural diversity studied by IR spectroscopy, PLoS One, (2014).

[30]P. Castellano, G. Vignolo, R.N. Farias, J.L. Arrondo, R. Chehin, Molecular view by fourier transform infrared spectroscopy of the relationship between lactocin 705 and membranes: speculations on antimicrobial mechanism, Appl Env. Microbiol, 73 (2007) 415–420.

[31]A. Hammersley, FIT2D: An Introduction and Overview, (1997).

[32]B.N. Ames, V.G. Elizabeth F. Neufeld, Assay of inorganic phosphate, total phosphate and phosphatases, in: Methods Enzymol., Academic Press, 1966: pp. 115–118.

[33]C.J. Minahk, L. Saavedra, F. Sesma, R. Morero, Membrane viscosity is a major modulating factor of the enterocin CRL35 activity, Biochimie, 87 (2005) 181–186.

[34]P. Garidel, A. Blume, Miscibility of phosphatidylethanolamine-phosphatidylglycerol mixtures as a function of pH and acyl chain length, Eur Biophys J, 28 (2000) 629–638.

[35]A. Blume, W. Hiibner, G. Messner, Fourier Transform Infrared Spectroscopy of13c=0-labeled Phospholipids Hydrogen Bonding To Carbonyl Groups, Biochemistry, (1988).

[36]R.N. Lewis, R.N. McElhaney, Calorimetric and spectroscopic studies of the polymorphic phase behavior of a homologous series of n-saturated 1,2-diacyl phosphatidylethanolamines, Biophys. J., (1993).

[37]Y.K. Levine, M.H.F. Wilkins, Structure of oriented lipid bilayers, Nat. New Biol., (1971).

[38]J.N. Israelachvili, Chapter 20 - Soft and Biological Structures, in: Intermol. Surf. Forces (Third Ed., Academic Press, San Diego, 2011: pp. 535–576.

[39]S.H. White, W.C. Wimley, A.S. Ladokhin, K. Hristova, Protein folding in membranes: Determining energetics of peptide-bilayer interactions, Methods Enzymol., (1998).

[40]E.J. Grasso, R.G. Oliveira, M. Oksdath, S. Quiroga, B. Maggio, Controlled lateral packing of insulin monolayers influences neuron polarization in solid-supported cultures, Colloids Surfaces B Biointerfaces, (2013).

[41]E.E. Ambroggio, G.D. Fidelio, Lipid-like behavior of signal sequence peptides at air-water interface, Biochim. Biophys. Acta - Biomembr., (2013).

[42]S.R. Dennison, L.H. Morton, F. Harris, D.A. Phoenix, Low pH Enhances the Action of Maximin H5 against Staphylococcus aureus and Helps Mediate Lysylated Phosphatidylglycerol-Induced Resistance, Biochemistry, (2016).

[43]M. Eeman, A. Berquand, Y.F. Dufrêne, M. Paquot, S. Dufour, M. Deleu, Penetration of surfactin into phospholipid monolayers: Nanoscale interfacial organization, Langmuir, (2006).

[44]K. Lohner, A. Latal, G. Degovics, P. Garidel, Packing characteristics of a model system mimicking cytoplasmic bacterial membranes, Chem Phys Lipids, 111 (2001) 177–192.

[45]P. Wydro, K. Witkowska, The interactions between phosphatidylglycerol and phosphatidylethanolamines in model bacterial membranes: the effect of the acyl chain length and saturation, Colloids Surf B Biointerfaces, 72 (2009) 32–39.

[46]P. Wydro, M. Flasiński, M. Broniatowski, Molecular organization of bacterial membrane lipids in mixed systems - A comprehensive monolayer study combined with Grazing Incidence X-ray Diffraction and Brewster Angle Microscopy experiments, Biochim. Biophys. Acta - Biomembr., (2012).

[47]M.R. Rintoul, R.D. Morero, F.G. Dupuy, The antimicrobial peptide microcin J25 stabilizes the gel phase of bacterial model membranes, Colloids Surfaces B Biointerfaces, 129 (2015) 183–190.

[48]L. Picas, C. Suárez-Germà, M.T. Montero, Ò. Domènech, J. Hernández-Borrell, Miscibility behavior and nanostructure of monolayers of the main phospholipids of escherichia coli inner membrane, Langmuir, (2012).

[49]R.M. Epand, R.F. Epand, Lipid domains in bacterial membranes and the action of antimicrobial agents, Biochim Biophys Acta, 1788 (2009) 289–294.

[50]C. Ratledge, S.G. Wilkinson, Microbial lipids, Academic Press, London, 1989.

[51]N. Malanovic, K. Lohner, Gram-positive bacterial cell envelopes: The impact on the activity of antimicrobial peptides, Biochim. Biophys. Acta - Biomembr., (2016).

[52]R.V.V. Tatituri, B.J. Wolf, M.B. Brenner, J. Turk, F.F. Hsu, Characterization of polar lipids of Listeria monocytogenes by HCD and low-energy CAD linear ion-trap mass spectrometry with electrospray ionization, Anal. Bioanal. Chem., (2015).

[53]S.K. Mastronicolis, J.B. German, G.M. Smith, Diversity of the polar lipids of the food-borne pathogen Listeria monocytogenes, Lipids, (1996).

[54]Y.-M. Zhang, C.O. Rock, Membrane lipid homeostasis in bacteria, Nat. Rev. Microbiol., (2008).

[55]R.N.A.H. Lewis, R.N. McElhaney, The physicochemical properties of cardiolipin bilayers and cardiolipin-containing lipid membranes, Biochim. Biophys. Acta - Biomembr., (2009).

[56]G. Carranza, F. Angius, O. Ilioaia, A. Solgadi, B. Miroux, I. Arechaga, Cardiolipin plays an essential role in the formation of intracellular membranes in Escherichia coli, Biochim. Biophys. Acta - Biomembr., (2017).

[57]R.P. Rand, S. Sengupta, Cardiolipin forms hexagonal structures with divalent cations, BBA - Biomembr., (1972).

[58]K. Thedieck, T. Hain, W. Mohamed, B.J. Tindall, M. Nimtz, T. Chakraborty, J. Wehland, L. Jänsch, The MprF protein is required for lysinylation of phospholipids in listerial membranes and confers resistance to cationic antimicrobial peptides (CAMPs) on Listeria monocytogenes, Mol. Microbiol., (2006).

[59]J.F. Tocanne, P.H.J.T. Ververgaert, A.J. Verkleij, L.L.M. van Deenen, A monolayer and freeze-etching study of charged phospholipids I Effects of ions and pH on the ionic properties of phosphatidylglycerol and lysylphosphatidylglycerol, Chem. Phys. Lipids, (1974).

[60]S. Danner, G. Pabst, K. Lohner, A. Hickel, Structure and thermotropic behavior of the staphylococcus aureus lipid lysyl-dipalmitoylphosphatidylglycerol, Biophys. J., (2008).

[61]J. Pan, F.A. Heberle, S. Tristram-Nagle, M. Szymanski, M. Koepfinger, J. Katsaras, N. Kučerka, Molecular structures of fluid phase phosphatidylglycerol bilayers as determined by small angle neutron and X-ray scattering, Biochim. Biophys. Acta - Biomembr., (2012).

[62]E. Salvucci, E.M. Hebert, F. Sesma, L. Saavedra, Combined effect of synthetic enterocin CRL35 with cell wall, membrane-acting antibiotics and muranolytic enzymes against Listeria cells, Lett. Appl. Microbiol., (2010).

[63]F.G. Dupuy, B. Maggio, N-acyl chain in ceramide and sphingomyelin determines their mixing behavior, phase state, and surface topography in langmuir films, J. Phys. Chem. B, 118 (2014) 7475–7487.

[64]P. Calvez, S. Bussières, Éric Demers, C. Salesse, Parameters modulating the maximum insertion pressure of proteins and peptides in lipid monolayers, Biochimie, (2009).

[65]E. Van Den Brink-Van Der Laan, J. Antoinette Killian, B. De Kruijff, Nonbilayer lipids affect peripheral and integral membrane proteins via changes in the lateral pressure profile, Biochim. Biophys. Acta - Biomembr., (2004).

[66]V. Castelletto, R.H. Barnes, K.A. Karatzas, C.J.C. Edwards-Gayle, F. Greco, I.W. Hamley, R. Rambo, J. Seitsonen, J. Ruokolainen, Arginine-Containing Surfactant-Like Peptides: Interaction with Lipid Membranes and Antimicrobial Activity, Biomacromolecules, (2018).

[67]C.M. Ernst, P. Staubitz, N.N. Mishra, S.J. Yang, G. Hornig, H. Kalbacher, A.S. Bayer, D. Kraus, A. Peschel, The bacterial defensin resistance protein MprF consists of separable domains for lipid lysinylation and antimicrobial peptide repulsion, PLoS Pathog., (2009).

[68]S. Vanounou, A.H. Parola, I. Fishov, Phosphatidylethanolamine and phosphatidylglycerol are segregated into different domains in bacterial membrane A study with pyrene-labelled phospholipids, Mol Microbiol, 49 (2003) 1067–1079.

[69]H. Strahl, J. Errington, Bacterial Membranes: Structure, Domains, and Function, Annu. Rev. Microbiol., (2017).

[70]J. V. Busto, A.B. García-Arribas, J. Sot, A. Torrecillas, J.C. Gómez-Fernández, F.M. Goñi, A. Alonso, Lamellar gel (Lβ) phases of ternary lipid composition containing ceramide and cholesterol, Biophys. J., (2014).

[71]A. Serio, M. Chiarini, E. Tettamanti, A. Paparella, Electronic paramagnetic resonance investigation of the activity of Origanum vulgare L essential oil on the Listeria monocytogenes membrane, Lett. Appl. Microbiol., (2010).

[72]M.B. Najjar, M. Chikindas, T.J. Montville, Changes in Listeria monocytogenes membrane fluidity in response to temperature stress, Appl. Environ. Microbiol., (2007).

[73]P. Hingston, J. Chen, K. Allen, L.T. Hansen, S. Wang, Strand specific RNA-sequencing and membrane lipid profiling reveals growth phase-dependent cold stress response mechanisms in Listeria monocytogenes, PLoS One, (2017).

[74]P.R. Cullis, M.J. Hope, C.P.S. Tilcock, Lipid polymorphism and the roles of lipids in membranes, Chem. Phys. Lipids, (1986).

[75]J.M. Seddon, G. Cevc, R.D. Kaye, D. Marsh, X-ray diffraction study of the polymorphism of hydrated diacyl- and dialkylphosphatidylethanolamines, Biochemistry, 23 (1984) 2634–2644.

[76]E.F. Haney, S. Nathoo, H.J. Vogel, E.J. Prenner, Induction of non-lamellar lipid phases by antimicrobial peptides: a potential link to mode of action, Chem. Phys. Lipids, (2010).

[77]E.J. Prenner, R.N.A.H. Lewis, K.C. Neuman, S.M. Gruner, L.H. Kondejewski, R.S. Hodges, R.N. McElhaney, Nonlamellar phases induced by the interaction of gramicidin S with lipid bilayers A possible relationship to membrane-disrupting activity, Biochemistry, (1997).

[78]P.C.A. Van Der Wel, T. Pott, S. Morein, D. V. Greathouse, R.E. Koeppe, J.A. Killian, Tryptophan-anchored transmembrane peptides promote formation of nonlamellar phases in phosphatidylethanolamine model membranes in a mismatch- dependent manner, Biochemistry, (2000).

[79]M. Zasloff, Antimicrobial peptides of multicellular organisms, Nature, (2002).

[80]K.A. Brogden, Antimicrobial peptides: Pore formers or metabolic inhibitors in bacteria?, Nat. Rev. Microbiol., (2005).

[81]A. Marquette, B. Bechinger, Biophysical investigations elucidating the mechanisms of action of antimicrobial peptides and their synergism, Biomolecules, (2018).

[82]N.L. Fregeau Gallagher, M. Sailer, W.P. Niemczura, T.T. Nakashima, M.E. Stiles, J.C. Vederas, Three-dimensional structure of leucocin a in trifluoroethanol and dodecylphosphocholine micelles: Spatial location of residues critical for biological activity in type IIa bacteriocins from lactic acid bacteria, Biochemistry, (1997).

[83]H.S. Haugen, G. Fimland, J. Nissen-Meyer, P.E. Kristiansen, Three-dimensional structure in lipid micelles of the pediocin-like antimicrobial peptide curvacin A, Biochemistry, (2005).

[84]F. Bédard, I. Fliss, E. Biron, Structure-Activity Relationships of the Bacteriocin Bactofencin A and Its Interaction with the Bacterial Membrane, ACS Infect. Dis., (2019).

[85]S. Castano, B. Desbat, A. Delfour, J.M. Dumas, A. Da Silva, J. Dufourcq, Study of structure and orientation of mesentericin Y105, a bacteriocin from Gram-positive Leuconostoc mesenteroides, and its Trp-substituted analogues in phospholipid environments, Biochim. Biophys. Acta - Biomembr., (2005).

[86]J.M. Seddon, R.H. Templer, A.J. Hoff, Chapter 3 - Polymorphism of Lipid-Water Systems, in: R.L. and E. Sackmann (Ed.), Handb. Biol. Phys., First, North-Holland, Amsterdam, 1995: pp. 97–160.

[87]S. Gruner, Lipid Polymorphism: The Molecular Basis of Nonbilayer Phases, Annu. Rev. Biophys. Biomol. Struct., (1985).

[88]J.M. Seddon, Structure of the inverted hexagonal (HII) phase, and non-lamellar phase transitions of lipids, Biochim Biophys Acta, 1031 (1990) 1–69.

[89]G.N. Moll, W.N. Konings, A.J.M. Driessen, Bacteriocins: Mechanism of membrane insertion and pore formation, in: Antonie van Leeuwenhoek, Int. J. Gen. Mol. Microbiol., 1999.

[90]M. Kjos, J. Borrero, M. Opsata, D.J. Birri, H. Holo, L.M. Cintas, L. Snipen, P.E. Hernández, I.F. Nes, D.B. Diep, Target recognition, resistance, immunity and genome mining of class II bacteriocins from Gram-positive bacteria, Microbiology, (2011).

Graphical abstract

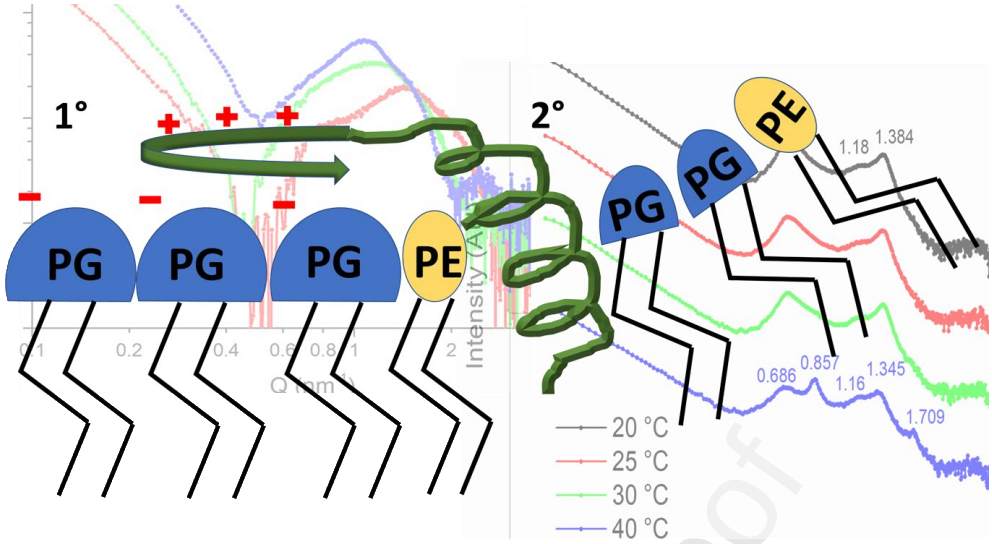

Highlights

Enterocin CRL35 is a 43 residues bacteriocin active against foodborne *Listeria monocytogenes*;

PG:PE lipid mixtures with different acyl chain length were prepared for studying membrane fluidity and structure upon peptide interaction;

The bacteriocin permeabilizes membranes and induces non-bilayer structures;